16th International Conference on Space Operations, Cape Town, South Africa – 3 - 5 May 2021.

SpaceOps-2021,7,x1386

ATTITUDE CONTROL on GRACE FOLLOW-ON
Experiences from the first years in orbit

F. Cossavella [a]*, J. Herman[b], L. Hoffmann[c], D. Fischer[d], B. Schlepp[e], T. Usbeck[f]

[a] *Deutsches Zentrum für Luft- und Raumfahrt e.V. (DLR), Germany*, Fabiana.Cossavella@dlr.de
[b] *Deutsches Zentrum für Luft- und Raumfahrt e.V. (DLR) (retired), Germany*, anja.herman@t-online.de
[c] *Deutsches Zentrum für Luft- und Raumfahrt e.V. (DLR), Germany*, L.Hoffmann@dlr.de
[d] *Airbus Defence and Space - Space Systems, Germany*, Denis.Fischer@airbus.com
[e] *Deutsches Zentrum für Luft- und Raumfahrt e.V. (DLR), Germany*, Benjamin.Schlepp@dlr.de
[f] *Airbus Defence and Space - Space Systems, Germany*, Thomas.Usbeck@airbus.com

* Corresponding Author

Abstract

The two satellites for the GRACE* Follow-on mission were successfully launched in May 2018 on a polar orbit at an altitude of 491 km. The mission continues the measurements of the gravity field of the Earth (with emphasis on the time variability) and also delivers radio occultation measurements. The twin satellites are kept at a relative distance of 170 to 270 km and act as probes in the gravity field of the Earth. The inter-satellite distance is measured by a microwave tracking system to an accuracy of 1 µm. A laser ranging interferometer is added as a technology demonstration. Stable and accurate relative pointing, as well as the minimization of disturbance torques, is required in order to optimize scientific results. This poses stringent demands upon attitude control. The performance of the GRACE Follow-on attitude control system will be presented, as well as the special actions and changes that became necessary as the mission evolved. A short description of the sensors and actuators used for attitude control is given and improvements with respect to GRACE are discussed in some more detail. The operational modes are described with a focus on the so-called nominal fine-pointing mode, in which the front-ends point towards each other in order to enable microwave- and laser-ranging. The third Section opens with a description of special tasks, such as the fine-tuning of the control and monitoring parameters and the complex determination of the satellite's center of gravity. A comparison is made with a tracking model based upon the fuel expenditure from the two tanks that can be determined independently. Several series of involved tests with manual thruster firings were performed in order to characterize the response of the accelerometers to thruster actuations. A description of the design of the tests, their execution and results is presented. A switch to the redundant instrument was made five months after launch on one of the satellites. The consequences for attitude control are discussed in Section 4. A method that was developed to cope with a situation where also the redundant GPS receiver would become unavailable is discussed in detail. Conclusions and an outlook for the upcoming years of operations are presented in the last Section.

Keywords: GRACE-FO, AOCS

Acronyms/Abbreviations

Acquisition and Safe mode (ASM)
ASM Rate Damping (ASM-RD)
ASM Coarse Pointing (ASM-CP)
ASM Steady State (ASM-SS)
Attitude and Orbit Control System (AOCS)
Attitude Control Thruster (ACT)
Coarse Earth & Sun Sensor (CESS)
Cold Gas Propulsion System (CGPS)
Center of Mass (CoM)
Center of Mass Calibration (CMC)

* Gravity Recovery And Climate Experiment. The predecessor GRACE was launched in 2002 and operated by the same partners until 2017

Deutsches Zentrum für Luft- und Raumfahrt (DLR) – German Aerospace Center
Failure Detection, Isolation and Recovery (FDIR)
Flight Dynamic System (FDS)
Fluxgate Magnetometers (FGM)
GeoForschungsZentrum (GFZ) – German Research Center for Geosciences
Global Positioning System (GPS)
Gravity Recovery And Climate Experiment (GRACE)
Grace Follow-on (GRACE-FO)
Grace Follow-on 1 (GF1)
Grace Follow-on 2 (GF2)
German Space Operations Center (GSOC)
Inertial Measurement Unit (IMU)
Instrument Processing Unit (IPU)
Jet Propulsion Laboratory (JPL)
Launch and Early Orbit Phase (LEOP)
Laser Ranging Interferometer (LRI)
Magnetic Torquers (MTQ)
Normal Mode (NOM)
On-Board Computer (OBC)
Orbit Control Mode (OCM)
Orbit Control Thruster (OCT)
Orbit Determination (OD)
On-board Orbit Propagator (OOP)
Pressure-Volume-Temperature (PVT)
Radial Tangential Normal (RTN)
Start tracker (STR)
Start tracker head 1 (STR1)
Start tracker head 2 (STR2)
Start tracker head 3 (STR3)
Start tracker Electronic (STRE)
Two-Line Elements (TLEs)

1. Introduction

GRACE Follow-On is a scientific co-operation between the USA and Germany, following the model initiated by its predecessor GRACE [1, 2]. The twin satellites were built by Airbus Defence and Space in Germany, under a contract from NASA's Jet Propulsion Laboratory (JPL). Operations are carried-out at the German Space Operations Center (DLR-GSOC) on behalf of the German Research Center for Geosciences (GFZ).

The main scientific goal of the mission is to collect data for creating both static and time-varying maps of the terrestrial gravity field. The satellites were launched in May 2018 at an altitude of 491 km on a circular polar orbit. They are kept at a relative distance of 170 to 270 km and act as probes in the gravity field of the Earth. The inter-satellite distance is measured by a microwave tracking system to an accuracy of 1 μm, a laser ranging instrument (LRI) is added as a technology demonstration and has improved the accuracy of the distance measurements by a factor of 30 [3, 4]. Non-gravitational disturbances can be determined with a SuperStar accelerometer.

The front-ends of the satellites have to point towards each other to enable microwave- and laser-ranging. Stable and accurate relative pointing and the minimization of disturbance torques are required in order to optimize scientific results. This poses stringent demands upon attitude control.

A short description of the sensors and actuators of the attitude and orbit control system (AOCS) is given in the next section. Improvements with respect to GRACE are discussed in some more detail, in particular those for the star cameras and the inertial measurement units.

The performance of the AOCS during nominal operation is evaluated based on the data collected during the first two and a half years in orbit. A description of several special activities necessary to improve the analysis of the scientific data is given with particular emphasis on the consequences for the attitude control of the satellite.

A switch to the redundant instrument was made five months after launch on one of the satellites [5]. This comprised not only a switch of the instrument processing unit, but also of the ultra-stable oscillator, GPS receiver, microwave assembly and electronics. The consequences for attitude control are discussed in the Section 4, together with a modified operational approach to bridge several months without on-board GPS data.

2. The Attitude and Orbit Control System

The design of the GRACE-FO satellites benefits from the experience gained from their predecessors. In particular the number and quality of the sensors has been improved [6]. A schematic view of one of the satellites is shown in Fig. 1, a detailed description of the satellite layout can be found in [2].

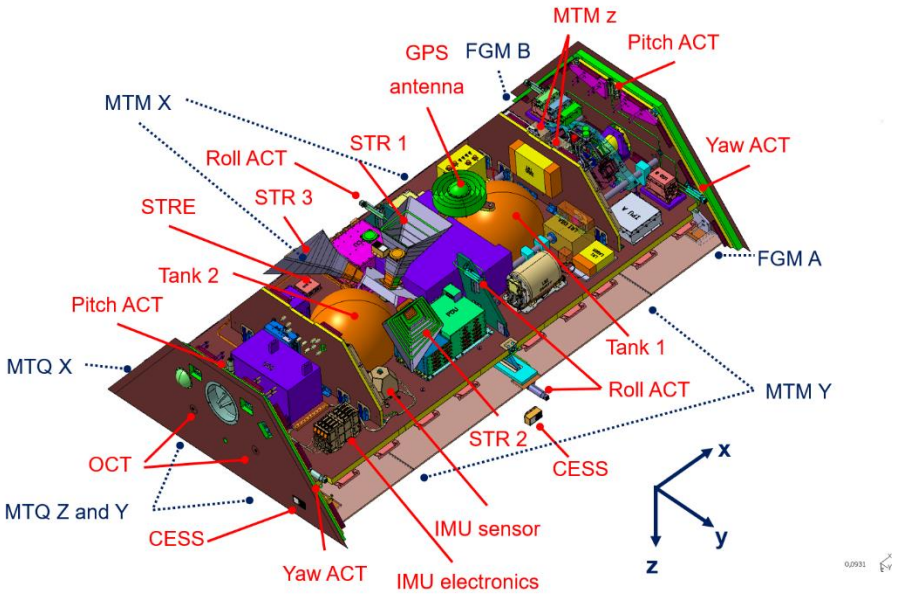

Fig. 1. Layout of one of the satellites (solar panels not shown). The location of the AOCS units is shown by red arrows. The dashed blue lines indicate the approximate location of units that are hidden.

The Coarse Earth & Sun Sensors (CESS) provides attitude measurements with respect to the direction of Sun and Earth. It consists of six sensor heads allocated along each axis, pair wise in opposite directions, in order to provide a spherical field of view. Each head consists of six thermistors, three for the detection of infrared light and three for the detection of Sun light, providing a 2-out-of-3 redundancy.

The magnetic field is measured by one of two fluxgate magnetometers (operated in cold redundancy) with an accuracy of 325 nT. Each magnetometer consists of three independent magnetic sensors aligned to the satellite axes and operating simultaneously. The measurements are input for control with the magnetic torque rods and are also used as back-up computation of the rotation rates in acquisition and safe mode.

The use of a high-performance Inertial Measurement Unit (IMU) with four independent axes provides accurate rate measurements. A tetrahedral configuration of the inertial sensors offers one-failure tolerance. Three sensors are used during nominal operations, the fourth only after a transition into safe mode. On GRACE a medium performance IMU with three measurement axes was available, providing no redundancy.

GRACE had two star cameras of which only one was actively used for AOCS. GRACE-FO has three star-tracker heads with a separation between their boresights of 80.4° to 100°. The three STRs are used in hot redundancy and are connected to one of two electronic units which are operated in cold redundancy. The data are handled by the on-board computer (OBC) directly, whereas on GRACE they were collected and processed by the instrument processing unit before being handed to the OBC for use by the AOCS. This configuration optimizes the coverage and increases the accuracy of the attitude measurement in all three satellite axes. The new generation of star cameras can handle partial Moon intrusions and the on-board software autonomously delivers fused attitude data from one, two or three cameras depending upon validity.

As on GRACE, GPS data are provided by a dual-band receiver and the data are handled by the processing unit of the microwave instrument (IPU). These data are used to initialize the on-board orbit propagator (OOP) at each AOCS cycle.

The attitude is controlled primarily by a set of cold redundant magnetic torque rods (MTQs) of 27.5 Am² each. Each rod has a double coil providing cold redundancy. The rods are aligned with the axes of the satellite and located at maximum distance from the magnetometers in order to minimize disturbances on the magnetic field measurements. The MTQs are supplemented by a cold gas propulsion system with a set of twelve 10 mN attitude control thrusters

(ACTs), separated into two branches. Two gas tanks of equal volume are mounted symmetrically along the x-axis of the spacecraft and are connected each to one of the branches, which are operated simultaneously to ensure an even depletion of the tanks. The design is inherited from GRACE with state-of-the-art enhancements and small improvements like a two-stage pressure regulator that assures a constant feed pressure for the thrusters over the whole range of tank pressures. Two orbit control thrusters of 50 mN thrust, located at the rear part of the satellite, complete the cold gas propulsion system.

2.1 Attitude modes and frames of reference

There are three main AOCS operation modes. The Acquisition and Safe Mode (ASM) is designed to guarantee power and thermal survival of the spacecraft, the Normal Mode (NOM) is the normal operating mode providing accurate three-axis attitude control according to the defined reference, and the Orbit Control Mode (OCM) is used for the necessary orbit change and maintenance maneuvers during the mission.

In addition, a reference attitude can be independently set by defining a frame of reference and a pointing bias. The pointing bias can be defined for each axis as Euler angle and it is added to the target attitude defined by the frame of reference.

The available frames of reference are the Nadir Pointing Frame, the Relative Pointing Frame and the Orbit Control Frame. In Nadir Pointing the z-axis of the satellite is aligned to the nadir direction, the y-axis is perpendicular to the plane defined by the z-axis and the velocity vector, and the x-axis is roughly pointed in the flight direction. The Orbit Control frame aligns the x-axis with the spacecraft velocity vector, the y-axis is perpendicular to the orbit plane and in the direction of the orbit normal vector. The z-axis completes the right-handed system.

As the horn antenna of the microwave instrument is located at the front of the satellite, in order to establish a link the two GRACE-FO spacecraft must point towards each other. When the Nadir frame is selected, a 180 deg yaw bias must be applied to rotate the leading satellite towards the trailing one. Precise inter-satellite pointing, however, is ensured only by selecting the Relative Pointing frame. This points the +x-axis to the other S/C, following a trajectory generated by an on-board algorithm according to an inter-satellite line of sight reference with the z-axis pointing towards Earth. The mutual distance is kept at 220±50 km, which leads to a continuous small pitch bias of roughly -1 deg. The slowly varying mutual distance implies that the desired attitude is not a constant. Therefore, each day the latest result of the orbit determination for both satellites are up-loaded to both satellites in form of Two-Line-Elements (TLEs).

Attitude biases around the pitch and roll axes are nominally not commanded, and used only during the calibration of the K-Band antenna pattern.

2.1.1 Acquisition and Safe Mode

ASM is autonomously entered after a mode drop by FDIR from the higher attitude modes, or after an on-board computer boot. The mode is divided into three sub-modes: rate damping (RD), coarse pointing (CP) and steady state (SS).

The ASM-RD is the point of entry of the ASM, the main task is to reduce the satellite rates to less than 0.2 deg/s, no control of the attitude is performed. The spacecraft rotation rate is measured by the IMU or derived from CESS and magnetometer measurements in case of non-availability of IMU data.

In ASM-CP a coarse nominal pointing of the S/C is achieved, with the z-axis of the satellite directed towards Earth and a yaw angle of 0° or 180°, depending on which value is closer to the current attitude.

The ASM-SS keeps the spacecraft in a coarse Earth-pointing attitude. The more powerful battery on GRACE-FO (78Ah name-plate capacity on GRACE-FO compared to 18Ah on GRACE) tolerates temporary yaw deviations of up to 60° in safe mode. No "yaw-steering" concept [7], forcing one of the side panels towards the Sun, is applied on GRACE-FO in ASM-SS.

The ASM mode intrinsically uses the Nadir Pointing frame as reference.

2.1.2 Normal Mode

NOM is the normal operating mode and it provides accurate Earth-pointing attitude according to the defined reference. The reference attitude is derived from the spacecraft position and velocity state vector provided by the GPS or, in case of a GPS outage, by an AOCS on-board orbit propagator.

The normal mode is subdivided into an intermediate acquisition sub-mode (ACQ), the Attitude Hold (AH) and the Fine Pointing (FP) sub-modes.

The NOM-ACQ is the entry point of the normal mode from coarse pointing in ASM or from OCM. The spacecraft acquires a specified 3-axis attitude relative to the selected frame, with an accuracy better than 30 mrad at 3σ confidence level. Rotations of the spacecraft of 180° in yaw are always performed in this mode.

Attitude Hold is entered from NOM-ACQ or from the NOM-FP and it holds the reference 3-axis attitude, with an absolute pointing error (at 3σ confidence level) better than 10 mrad in roll, and better than 5 and 3 mrad in yaw and pitch respectively. The attitude hold mode is used for center of mass calibrations and any other special AOCS operation that could lead to not nominal attitude disturbances, as for example an update of the NOM-FP controller settings or specific thruster tests.

The NOM-FP is the mode that provides high accuracy attitude pointing for science operation. The roll axis is controlled with an accuracy better than 2 mrad, while the pitch and yaw axes are controlled with an accuracy better than 0.25 mrad at 3σ confidence level. A science configuration is established once the Relative Pointing is activated in NOM-FP.

The use of TLEs to point towards the partner satellite is on GRACE-FO not restricted to the fine pointing (science) mode. This can be set by command in any NOM sub-mode, thus allowing for extra flexibility when performing special tests.

In all NOM sub-modes, the inertial attitude information is derived from accurate autonomous star sensor measurements and propagated to the current on-board time using measurements of the spacecraft rate from the high accuracy IMU. Attitude measurements from at least two star sensors are fused together, in order to achieve low noise in all axes by eliminating the star sensor boresight noise, which is typically 10 times higher than the cross-axis noise.

The spacecraft rate is also derived from star sensor measurements, as back-up in case of non-availability of IMU data. The CESS is used for FDIR surveillance of Sun/Earth angles in the normal mode.

Actuation is performed mainly by the magnetic torquers, augmented by the cold gas thrusters whenever necessary. The thrusters are operated with different sets of thrust limitation parameters according to the actual state of the attitude and rate errors. Magnetorquer control is based on on-board magnetometer measurements. The NOM-AH mode reflects the GRACE Attitude Hold Mode except for orbit control maneuvers and the NOM-FP mode the GRACE Science Mode [7].

2.1.3 Orbit Control Mode

This mode is used for the necessary orbit change and maintenance maneuvers during the mission under direct ground control. It provides the same principal functionality as the NOM-AH mode and uses the same equipment plus the orbit control thrusters, which are disabled in NOM. The OCM has no sub-modes.

2.2 AOCS performance

The AOCS on GRACE-FO has shown a very stable behavior since launch. Both satellites have been commanded to NOM-FP ~21h after separation; GF1 and GF2 have since then maintained fine pointing for more than 98% and 93% of the time, respectively.

The science configuration, i.e. simultaneous NOM-FP and Relative Pointing on both satellites, has been maintained for 86% of the mission life time. It was interrupted by maintenance phases to execute specific AOCS activities or orbit maneuvers, and by AOCS safe modes.

In order to maintain the twin satellites within a relative distance of 220±50 km, five orbit control maneuvers were executed on GF1 and six on GF2, one of which was a collision avoidance maneuver in 2018.

The longest interruptions of the science configuration were two prolonged periods in ASM and NOM-Nadir-Pointing on GF2, caused by an outage of the prime instrument processing unit in 2018 that left the AOCS without GPS data for a few months (see section 4) and by an OBC switch to the back-up unit in early 2019 [8]. GF2 has spent a total of ~32 days in ASM, GF1 less than 5. Fuel consumption on GRACE-FO is considerably smaller than it was for GRACE, although the pointing performance is considerably better [3, 6]. In ASM an average gas consumption of 2.5 g/day and 5 g/day has been observed on GF1 and GF2 respectively, smaller than the initially allocated budget of 30 g/day and with some variations according to the angle of the Sun with respect to the orbital plane. The nominal modes perform also better on GRACE-FO than on GRACE, with an average expenditure for both satellites of about 0.7 g/day in fine pointing mode (cf. 3 – 5 g/d in the equivalent Science Mode on GRACE) and ~1 g/day in attitude hold mode (cf. 10 g/d in Attitude Hold Mode on GRACE).

The GRACE-FO satellites were launched with ~32 kg nitrogen gas and have consumed in the first 2.5 years of life about 1.2 kg of fuel, leading to a life expectancy of more than 60 years based on the current fuel consumption.

2.2.1 Fuel consumption

Two methods are used to track the accumulated gas expenditure: the book-keeping method and the Pressure-Volume-Temperature (PVT) method.

The book-keeping is based on precise tracking of the total amount of time each thruster has been activated, and on knowledge of the thruster feed pressure and mass flow rate of each thruster unit. The mass flow rates at a reference

feed pressure of 1.5 bar are known from ground thruster calibrations, while the thruster on-times are recorded on board with one millisecond precision. The feed pressure in each propulsion branch is also available in the spacecraft telemetry. As the mass flow rates scale linearly with the feed pressure, it is possible to track how much gas has been ejected by each thruster over time.

The PVT method uses a combination of on-board and ground information together with the equation of state for a real gas to estimate the amount of mass in each pressure vessel:

$$m = \frac{P \cdot V}{R \cdot T \cdot Z}$$

where P is the pressure of the tank, V its volume, T its temperature, R is the universal gas constant and Z is the compressibility factor. Temperature and pressure of each tank are available in the on-board telemetry, while the volume of the vessel has been measured on ground before launch. In this work, a modified van der Waals approach to estimate the compressibility factor is used. The accuracy in the measurement of the gas temperature and pressure is the main source of uncertainty in this method, which can estimate the propellant mass with an accuracy of a few percent. Because the temperature sensors are located on the outer surface of the vessels, the PVT method does not provide accurate results during phases of fast cooling and heating of the nitrogen gas.

The book-keeping method is more suitable for calculating the consumption of the propellant mass but it is less sensitive to small leakages in the system. A comparison between the two methods is used as an indicator for leaks in the propulsion system. In Fig. 2 the estimated propellant expenditure for both tanks on each satellite is shown. The book-keeping method estimates on both satellites a slightly higher consumption of gas from tank 2 (located along the minus x-axis) because of the higher average feed pressure measured on the corresponding branch. The trend is confirmed by the results of the PVT mass estimation for all tanks, within the method uncertainties. On GF1, however, a small divergence between the two methods has been observed in the second half of 2020 and it is currently being investigated.

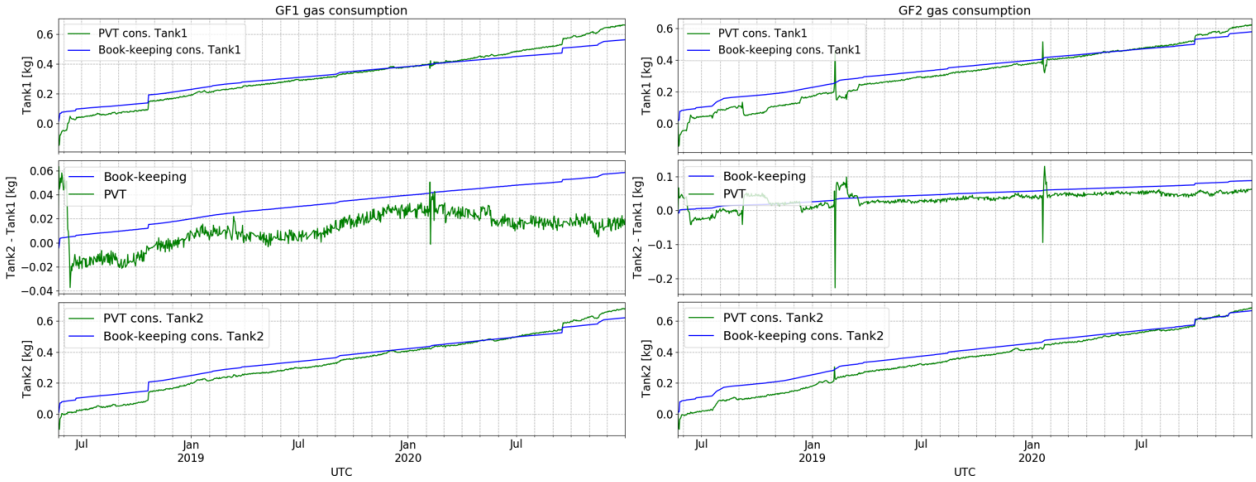

Fig. 2. Expenditure of gas on GF1 (left figure) and GF2 (right figure) as estimated with the PVT and book-keeping methods. The consumption of gas from tank 1 and tank 2 is displayed on the top and bottom panels, respectively. In the middle panel the difference in gas consumption between the two tanks is shown. Both satellites have consumed about 1.2 kg of nitrogen gas, with 25 to 60 grams more gas taken from tank 2 with respect to tank 1. Spikes in the used mass estimated from the PVT method coincide with fast cooling phases that followed the switch-off of both science instruments. This happened on GF2 in early 2019 and early 2020, and on GF1 in early 2020. The effect is stronger on tank 1, because it is closer to the instruments that are located at the front-end of the satellite.

2.2.2 Star tracker performance

The boresight of STR1 is close to the -z-axis of the satellite, while the boresight of STR2 and STR3 is close to the +y and -y-axis respectively (see Fig. 1). The use of three instead of two camera heads (as in GRACE) improves the attitude data availability and accuracy about all spacecraft axes. Fused data from all three heads were delivered for approximatively 70% of the time in the first two and a half years of the mission, whereas 0.2% of the time attitude data were derived from a single head only (the other two being blinded by the Sun and the Moon simultaneously; see Table 1). The individual heads deliver valid data for 87 - 94% of the time.

Table 1. Percentage of quaternion samples derived from the fusion of the data from 3, 2 or 1 star tracker heads (on top) and percentage of valid samples delivered by each star tracker head (on the bottom) with respect to the unit on-time, after 2.5 years in orbit.

	% of on-time	
	GF1	GF2
Fusion type:		
3 star cameras	71.06	69.94
2 star cameras	28.77	29.19
1 star camera	0.17	0.17
Validity:		
STR 1	93.95	93.28
STR 2	87.70	86.86
STR 3	89.17	88.25

Since GF1 flies backwards, i.e. with a 180° yaw bias with respect to the Nadir frame, the performance of GF1 STR2 has to be compared to that of STR3 on GF2. The same applies for GF1 STR3 and GF2 STR2.

The precession of the orbital plane has an inertial period of about 320 days (β´ cycle), implying that for ~160 days the Sun is on one side and for ~160 days on the other side of the satellite. β´ denotes the angle between the orbital plane and the direction to the Sun.

The behavior of each head depends on the phase in the β´cycle. STR1 is blinded by Sun for β´ around 0° (phase = 0.0 and 0.5), GF1 STR3 and GF2 STR2 are blinded by Sun for β´ around -90° (phase = 0.75), while for GF1 STR2 and GF2 STR3 this happens as β´ approaches +90° (phase = 0.25) (see Fig. 3).

The slightly lower performance of GF2 STR2, as compared to GF1 STR3, is due to an anomalous behavior of the star tracker head in January 2019, when 90% of the measurements were invalid. Although the satellites were going through their first β´ minimum phase, the same behavior was not observed on GF1 STR3. The anomaly was most likely caused by condensation on the lens of the star tracker 2 head. This hypothesis is confirmed by the nominal behavior of the star tracker head, when the same phase of the β´cycle was reached in the following cycles (see Fig. 3).

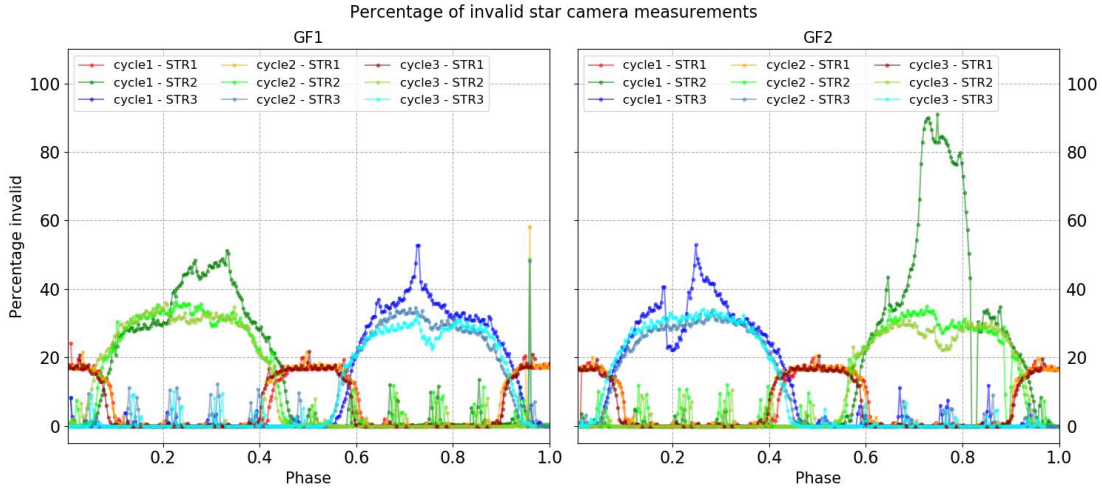

Fig. 3. Percentage of daily invalid star tracker measurements for each STR head as a function of the phase in the β´cycle. The performance of the STR for GF1 and GF2 is displayed, on the left and right panels respectively. The small peaks with 10% of invalid points occurring every month on both satellites are due to intrusion of the Moon in the field of view of the star cameras. The high number of invalid STR2 samples during cycle one on GF2, starting at a phase = 0.7, is associated to a condensation on the lens of the camera. The deep at a phase = 0.2 on GF2 during cycle one is due to a prolonged period in ASM, when the yaw angle was not controlled to a high precision and the camera was less often blinded by Sun than the corresponding head on GF1.

The alignment of each star camera head to the spacecraft frame of reference was determined on ground before launch [2]. Once in orbit, the relative alignment between the STR heads has been measured from the attitude data. The

zenith star camera was chosen as a reference. For the side STR sensors, the angle between the in-flight and on-ground calibrated mounting quaternions has been found to be between 0.4 and 0.6 mrad for each analysed quaternion pair. Attitude disturbances have been observed on both satellites when a STR head is excluded from the fusion process, usually because blinded by Sun or Moon. The effect is best visible when two out of three heads are simultaneously excluded and only one of the side cameras remains available. Attitude errors of about 0.5 mrad and occasionally up to 1 mrad were observed on the pitch axis in such cases, while nominally the pitch axis is controlled to better than 0.3 mrad. Although this level of disturbance is completely within the control capability of the NOM-FP mode, it led to a higher number of MTQ and pitch thruster actuations and could potentially disturb the science measurements.

To ensure a smoother transition between star tracker heads, the STR2 and STR3 alignments were updated on both satellites in June 2020. The analysis of the attitude errors after the star camera alignments have been updated indicates that the existing bias has been significantly reduced, although there is an intrinsic lower accuracy when only one camera head is used. Almost two years of data have been analysed, starting in March 2019. The data set has been divided into 5 sub-sets based on the number of star camera heads available for attitude determination. For each sub-set, the average attitude error along each axis was calculated before and after the update of the star tracker alignments. Only days with nominal attitude and no special AOCS activities have been selected, resulting in a total of roughly 430 days before and 255 days after the update. The result for the pitch axis is shown in Fig. 4. The corresponding mean and standard deviation are reported in Table 2. Before the alignments update on GF1, the average pitch error was -0.29 mrad when only measurements from STR2 were available, and 0.12 mrad when only measurements from STR3 were available. In contrast, when all cameras were available the average attitude error was -0.05 mrad. After the update, the average changed to 0.02 mrad and -0.10 mrad for the case in which only STR2 and only STR3 were valid, respectively. The standard deviation of the errors instead did not improve, because this is not due to a misalignment of the corresponding star cameras, rather to the lower accuracy of the measurement from only one head. Similar results have been observed for GF2. For the roll and yaw axes an improvement was also observed, but it is less significant and therefore not discussed here.

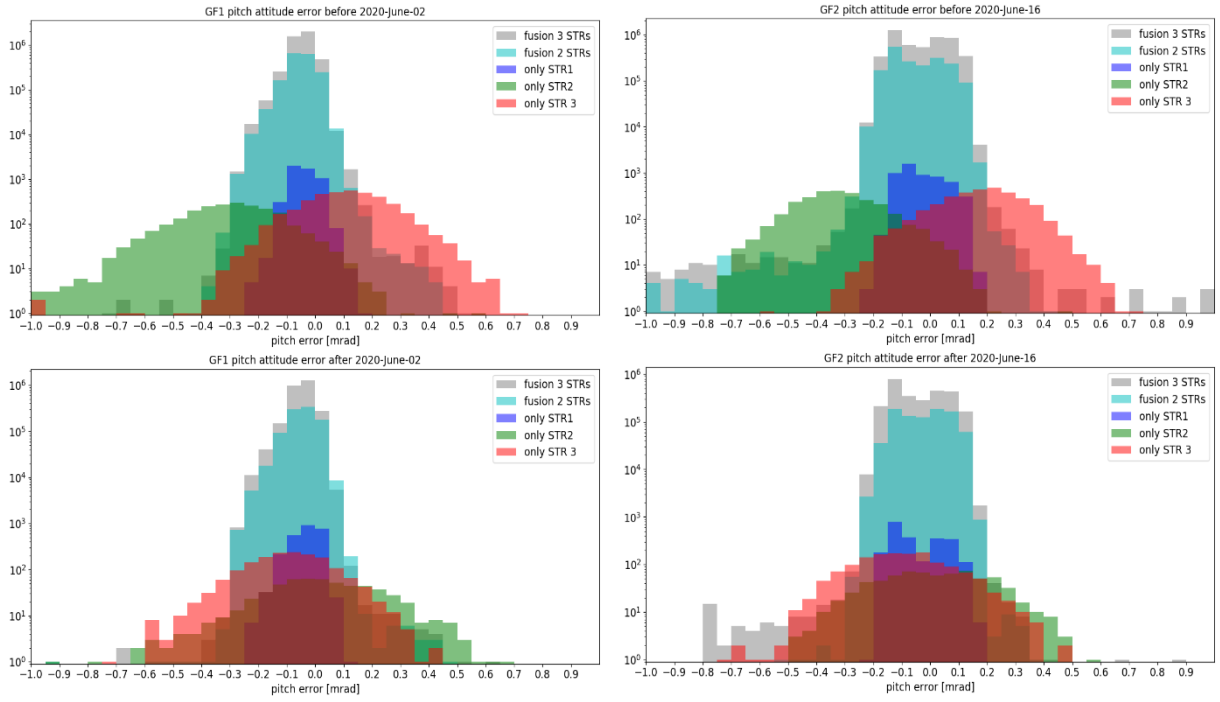

Fig. 4. Distribution of attitude errors along the pitch axis before (top panels) and after (bottom panels) the update of the alignment of the star trackers. On the left side are the attitude errors on GF1 and on the right side the GF2 ones. Due to the considerably smaller size of the data set corresponding to only one star camera head active, a logarithmic scale on the y-axis is used to better display all the five data sets at once. Five sets of data are depicted: in grey the attitude error when all STRs are available, in light blue when only two STRs are available and the case when only one star camera is delivering data is displayed in blue, green and red for STR1, STR2 and STR3, respectively.

Table 2. Mean and standard deviation of the attitude errors along the pitch axis, as a function of the number of star camera heads used in the fusion process. For each fusion type, values before and after the update of the star trackers alignement are reported.

		GF1		GF2	
Fusion Type		Before	After	Before	After
3 heads	Mean [mrad]	-0.05	-0.05	-0.03	-0.03
	std [mrad]	0.04	0.04	0.09	0.09
2 heads	Mean [mrad]	-0.04	-0.04	-0.04	-0.02
	std [mrad]	0.05	0.05	0.09	0.08
only head 1	Mean [mrad]	-0.03	-0.02	-0.04	-0.07
	std [mrad]	0.05	0.04	0.05	0.08
only head 2	Mean [mrad]	**-0.29**	**0.02**	**-0.34**	**-0.05**
	std [mrad]	0.17	0.21	0.12	0.18
only head 3	Mean [mrad]	**0.12**	**-0.10**	**0.18**	**-0.09**
	std [mrad]	0.15	0.19	0.15	0.17

3. Special activities

3.1 Center of mass calibration

Non-gravitational accelerations acting on the spacecraft have to be accurately measured in order to remove their effect on the measurement of the intersatellite distance. Therefore, each GRACE-FO spacecraft carries an accelerometer whose proof-mass is aligned to the center of mass (CoM) of the vehicle. Precise knowledge of the location of the center of mass and the capability of keeping it aligned within 100 µm to the proof-mass is required [2]. The satellite layout was optimized in order to control the offset between the CoM and the ACC proof mass to less than 500 µm in all axes. To keep the CoM offset within the desired range, each satellite is equipped with six movable mass trim mechanisms whose rails are parallel to the three axes of the satellite. Each mass weights ~5 kg and can be moved independently in steps of 2.5 µm, allowing for a compensation of the CoM offset up to ±2.16 mm along the x-axis and ±1.74 mm along the y- and z-axis.

The propellant tanks are located on the x-axis at the same distance from the CoM. An unequal fuel usage between them and leakages across the thruster branches are expected to induce over time a drift of the center of mass along the x direction.

The center of mass is measured in orbit by means of a center-of-mass calibration maneuver (CMC). A detailed description of its design and of the analysis method to determine the CoM can be found in [9]. A CMC consists of a periodic angular acceleration along the desired axis imposed on the spacecraft using the magnetic torquers. A constant magnetic torque of ±0.01 Nm is commanded along the selected satellite axis, following a nearly square wave pattern with a pulse width of 5 seconds and a period of 12 seconds. Each maneuver consists of 15 of these cycles, for an overall maneuver duration of 180 seconds. The AOCS executes automatically the maneuver based on the commanded input parameters. Before the calibration starts, the attitude is stabilized by narrowing the dead-bands in all spacecraft axes to 0.5 mrad. These are then set to infinity during the maneuver, resulting in no closed loop attitude control and no usage of attitude thrusters. At the end of a maneuver the closed loop attitude control is resumed automatically. A complete CMC campaign consists of seven maneuvers, two about the roll-axis, two about the yaw-axis and three about the pitch-axis, executed at specific geographic locations.

Two calibration campaigns were executed soon after LEOP. Signature of outgassing in the accelerometer data and an unexpected drift of the center of mass along the x-axis were observed by the science data groups at the Jet Propulsion Laboratory of the Californian Institute of Technology and at the Center for Space Research (CSR) at the University of Texas (Austin). In order to monitor the shift of the center of mass over a complete β´ cycle, twelve more campaigns were executed on a monthly basis until October 2019. The offset measured along the x-axis can be compared to the offset expected from the unequal consumption of fuel from the two propellant tanks. The satellite has been modelled as a simple five bodies system, whose masses are approximated as point masses located along the x-axis at fixed distance from the CoM [10]. The five bodies are the propellant tanks, the two mass trim mechanisms located along the x-axis and the remaining satellite mass that is fixed and won't change over time. The position of the latter has been estimated by taking as reference a CoM offset measured in orbit. Given the initial outgassing of the satellite, the calibration in February 2019, after the spacecraft went through almost a complete β´ cycle and had been illuminated from all sides, has been chosen as reference. The offset of the CoM position calculated from the estimated fuel consumption in the tanks in general represents well the measured one, for both the book-keeping and the PVT methods (see Fig. 5 for GF1). The latter shows some higher fluctuations due to changes of tank pressure and temperature in the

different phases of the β´ cycle. In February 2020 the trim mass was moved on GF1 in order to maintain the CoM offset within the desired range of ±100 µm. The discrepancy observed in the fuel consumption estimated by the PVT and book-keeping methods (see section 2.2.1) is visible also in this analysis. However, the uncertainties associated with both methods have not been evaluated yet and further investigation is ongoing.

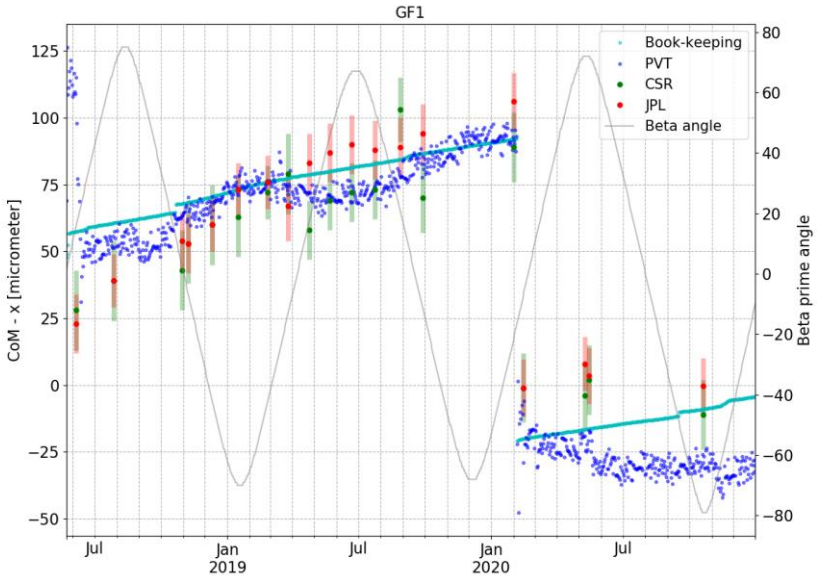

Fig. 5. Center of mass offset along the x-axis measured in orbit and estimated from the differential consumption of fuel in the propellant tanks on GF1. In red and green are the CoM offsets along the x-axis measured during the CMC campaigns and estimated from the JPL and CSR science teams, respectively. Superimposed is the estimation of the CoM offset due to the differential consumption of fuel as determined with the PVT (dark blue points) and book-keeping (light blue points) methods. The drop in February 2020 is due to a commanded movement of the trim mass to compensate for the accumulate offset. The discrepancy between the PVT and book-keeping methods in the second half of 2020 is currently under investigation. The β´ angle is displayed on the right axis.

3.2 Fine tuning of monitoring and control parameters

It was discovered soon after launch that the accelerometers on GRACE-FO display an improper response at short thruster firings, in particular at roll thruster firings [11]. Roll thruster activity is maximum at the geomagnetic equator, where the control authority of the magnetic torquers is drastically reduced in roll. Ways to reduce the overall thruster activity by making less but slightly larger pulses, thereby temporarily accepting larger deviations in roll, were investigated and tested. This was an iterative process that led to a total of three tests, each with a different combination of thruster and NOM-FP controller settings.

The first step was to modify only the settings for the commanding of the roll and yaw thrusters, including the increase of the minimum thruster on-time for the roll and yaw thrusters from 0.05 seconds to 0.5 and 0.075 seconds, respectively. The test performed as expected, the number of roll thruster firings was decreased by 85%, but the daily fuel expenditure increased by 50%. The attitude control performance was not affected.

In a second step the number of roll thruster actuations was even reduced by ~97% over a day. The minimum thruster on-time for the roll axis was increased to 1 second and for the yaw axis to 90 ms, and the angular dead bands for the two axes were increased to 5 mrad for roll and 0.5 mrad for yaw. The fuel consumption was higher than in the nominal configuration, but only by 34%. The extremely low fuel consumption on GRACE-FO provides enough margin to accept this moderate increase. However, also the number of pitch thruster firings increased (from 1 actuation per day, to 35 actuations per day), because of roll/pitch axis coupling through the deviation moment I_{xy}.

Finally, a third set of settings achieved a reduction of the roll thruster actuations by 95%, did not significantly increase the actuations in pitch axis and showed a fuel consumption comparable to what observed in the previous step. The maximum thruster on-time was increased to 1s for the roll thrusters and to 100 ms for the yaw and pitch ones, and the angular dead bands were enlarged for all axes. Overall no violation of the pointing requirements was observed. This third set of settings was maintained for about 3 months, from November 2018 until February 2019. Over this time

the performance could be estimated over a wider range of orbit conditions. It was observed that with the new configuration a longer stabilization time in the pitch axis was needed when switching between frames of reference. In February 2019, in wave of activities to recover GF2 from the OBC switch, it was decided to permanently revert all settings to defaults on both satellites and a method to calibrate the response of the accelerometer to the thruster actuations was investigated.

3.3 Tests to characterize the accelerometer response to thruster pulses

A series of thruster tests was executed to model the response of the accelerometers to the actuation of each ACT thruster [12]. Measurements of long pulses were recorded over a range of differential pressures between the two cold gas branches. This could be obtained by spacing out the thrusts by a predefined amount of time.

The backbone of each test is the capability to command the ACTs in open loop. On GRACE-FO it is possible to disable the AOCS control on the thrusters, an FDIR re-enables the on-board control after a configurable amount of time that is by default set to 300 seconds. During this period the ground operator can command a sequence of thruster activations along the selected axis. The test consists of a sequence of 20 to 60 ACT actuations, each one second long, spaced out by a variable amount of time that ranges between 2 seconds and 45 minutes. A different approach is used according to the length of the interval between subsequent thrusts. If the actuations are spaced by less than a minute, they are alternated along the same axis but in opposite directions in order to counteract the attitude deviation created by each single pulse. For sequences requiring some minutes between subsequent firings, the AOCS control on the thrusters is reactivated after each pulse and therefore there is no need to command an alternating sequence. With the thrusters being operated in open-loop, the attitude is controlled only through the MTQs. It is therefore advantageous to execute the tests at geographic locations where the magnetic torquer control authority is maximum for the axis along which the ACTs are being fired.

On GF1 a total of six tests was executed, with spacing between thrusts of 2 seconds and of 3, 10, 15, 30 and 45 minutes. All of them could be executed in NOM-FP over ten days, without interrupting the nominal science data acquisition and with attitude deviations of less than 1.5 mrad in pitch and yaw, and less than 4 mrad in roll. On GF2, a set of six tests was executed with spacing between thrusts of 2s, 4s ,7s, 11s, 21s and 15 minutes. Despite the alternating firing direction and the selection of the optimal geographic location, when commanding thrusts spaced by 4 to 21 seconds the attitude could drift and attitude errors up to 20 mrad in roll, 4 mrad in yaw and 1.5 mrad in pitch were observed. This part of the tests was therefore executed in the more robust attitude hold mode, resulting however in an interruption of the science mode for about six hours.

The complete set of tests was executed twice, in 2019 and 2020, and the data collected were used by the science data system to calibrate the output of the accelerometer before further using it in gravity field processing [12].

4. Operations without availability of GPS data

The data collected by GPS receiver are processed by the Instrument Processing Unit, which then provides to the AOCS the position, velocity and time measurements with a frequency of 0.5 Hz. This Position-Velocity-Time solution is propagated by the AOCS to the current on-board time by means of a fourth order gravity field model and a single step fourth order Runge Kutta algorithm. The resulting state vector is used for generating the reference attitude of the AOCS as described in section 2.1. The position and velocity information is additionally downloaded via the nominal telemetry stream and forwarded to the GSOC Flight Dynamics System (FDS) for the orbit determination of both S/C. The result of the orbit determination for both satellites is uplinked to each satellite every day in form of Two-Line Elements. These are used by the AOCS to determine the relative position with respect to the twin satellite and to perform an accurate inter-satellite pointing when the relative pointing frame of reference is selected.

In case of an IPU outage, the AOCS does not receive the GPS solution and by default propagates the last valid GPS measurement up to 24 hours. An on-board FDIR triggers an AOCS mode transition from NOM to ASM when this time period has expired. In order to cope with longer GPS or IPU outages in NOM, the on-board orbit propagator must be re-initialized periodically by uploading OOP files that contain the state vector for a given epoch. In absence of a GPS navigation solution, orbit data from SpaceTrack[†] in form of TLE files are used to generate the OOP files on ground. This process is shown in Fig. 6. Compared to the nominal process that uses the on-board GPS data, the use of SpaceTrack TLEs decreases the overall pointing accuracy of the AOCS. This depends mainly on the quality and frequency of the provided orbit data, the precision of the on-ground orbit determination and propagation performed by the FDS.

[†] https://www.space-track.org/

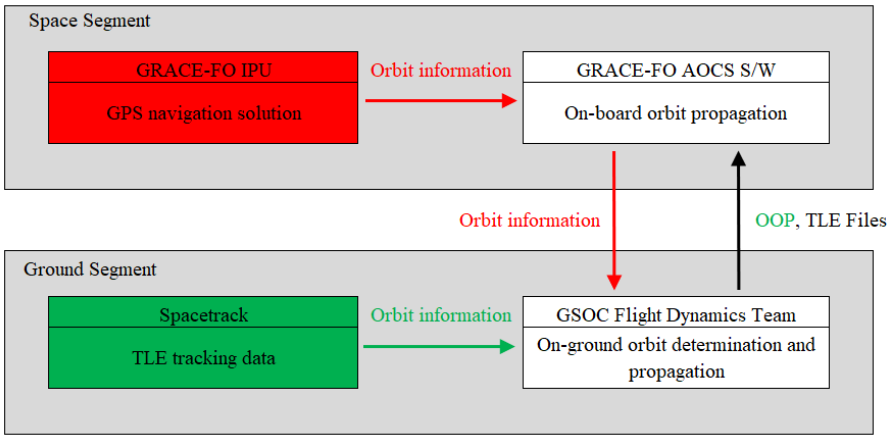

Fig. 6. Simplified processing and distribution flow of position and velocity information between the space segment and the ground segment of GRACE-FO. In case of a long GPS data outage (marked in red), the source of orbit information is changed to SpaceTrack TLEs (marked in green).

In 2018 the prime instrument processing unit on GF2 failed. During the months in which the switch to the redundant instrument chain was prepared, the AOCS was operated in normal mode and the nadir pointing frame of reference was selected. Orbit determination based on SpaceTrack TLE was performed on ground and OOP updates were uplinked to the satellite every two to three days. At every update, attitude errors in pitch of up to 4 mrad were observed. No attempt to maintain a relative inter-satellite pointing was done.

The following sub-section describes the method developed to cope with a long GPS data outage as well the analysis of the uncertainties associated with this method. The effect on the accuracy of the inter-satellite pointing is investigated in sections 4.2 and 4.3, in the worst-case scenario of the loss of the redundant instrument processing unit.

4.1. Improvement of on-ground orbit determination and propagation based on SpaceTrack TLE data

Between 2018-07-19 and 2018-10-16 no GPS navigation solution was available for GF2. The input for the on-ground calculation of the satellites orbit was therefore changed from GPS data to Spacetrack TLEs. This led to a higher uncertainty in the available orbit information that caused jumps of the relative position between GF1 and GF2 when applying updated TLEs data. The offset to the expected position was in the range of several kilometres. A modified approach to apply a fitting algorithm over several TLEs was therefore developed.

A set of two TLEs per day were downloaded for the previous 5 to 7 days and, by using a SGP4 propagator [13], an ephemeris from one TLE epoch to the next TLE epoch was created. These ephemerides were concatenated and handled as GPS navigation solution data, i.e. an orbit determination (OD) over that whole period was performed. Since the orbit determination comprises a batch least-squares fitting algorithm, the data of a single unprecise TLE was excluded by the OD process and an appropriately fitted orbit was obtained.

For a period of three months, from July 2019 until October 2019, the TLE-fitting algorithm was used in parallel to the nominal orbit determination process based on the on-board GPS navigation solution. The position offsets between GPS-based and TLE-based OD were calculated by propagating the result of both ODs to the same epoch until 24 hours after the generation time[‡]. The position offsets in the radial-tangential-normal frame[§] (RTN) were then compared over one orbit in order to evaluate the quality of the described approach. The result of this analysis over 103 days are given in Table 3. They show that the position offsets are slightly better but very similar to what obtained by using a single TLE [14], with the benefit that the standard deviation and the minimum/maximum outliers are much smaller using this new approach.

[‡] The OD results are used to provide on-board orbit products for the next 24 hours. The accuracy of these products should be of sufficient quality, which is why an analysis period of 24 hours was realized.

[§] Its origin is at the satellite position; the x-axis is aligned with the radial vector that points from the center of the Earth to the satellite (positive outwards), the z-axis is aligned to the normal direction perpendicular to the radial and velocity vector, and the y-axis completes the right-handed system pointing in the tangential direction.

Table 3. Statistics of position offset between an orbit determination based on GPS data and one based on a fitting algorithm over several TLEs in RTN-frame.

	R [m]	T [m]	N [m]
Minimum	-147	-3593	-163
Maximum	129	4271	163
Mean	0	10	0
1-Sigma	72	1480	57

The described TLE-fitting algorithm for the calculation of the satellites orbits requires periods without orbit maneuvers. For satellite missions performing orbit maneuvers on a daily basis, a different approach would have to be developed. This analysis was performed for a short period during a minimum in the solar flux cycle. The position offset between the two orbit determination methods can vary during different seasons and periods during the 11-year solar flux cycle, due to the changing atmospheric drag and solar pressure.

4.2. On-board propagation of position and velocity based OOP file updates provided from ground

Each satellite determines its own position and velocity using the data provided by the on-board GPS receiver. In case of an invalid GPS solution, the latest internally stored orbit state vector is propagated. This can be the last valid GPS solution or a manually commanded update of the on-board orbit propagator, which is based on ground generated products as described in the previous section.

An analysis of the overall errors associated with the approach described in 4.1 was performed over a period of three days, when the orbit determination based on both GPS measurements and SpaceTrack TLEs was available. The state vector derived by FDS from SpaceTrack TLEs and further propagated by the satellite on-board algorithms is compared to the position and velocity measured by the GPS receiver on board. The results are shown in Fig. 7. The error of the propagated position and velocity increases over time until the next ground commanded OOP update takes place. In this analysis a daily OOP update is executed at 17:00 UTC each day. Compared to the error in radial and normal direction, the position error in the tangential direction is significantly larger. The maximum velocity error, instead, is observed in radial direction. The smaller oscillations visible in the graphs are related to the position in orbit. A residual error remains after the execution of a new OOP update, due to the initial error induced by the SpaceTrack TLEs and the following on-ground propagation of the data to a future timestamp.

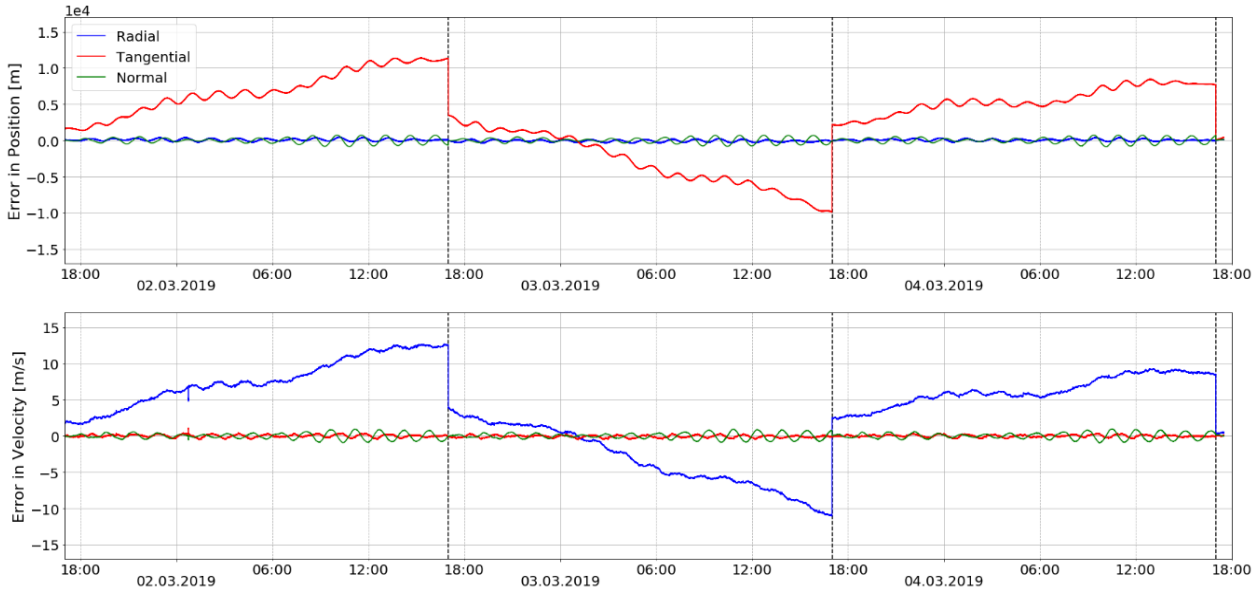

Fig. 7. Calculated position and velocity error in RTN-frame over a period of three days. The error is estimated by comparing the GPS measurements to the position and velocity calculated on board by propagating the daily OOP updates (based on SpaceTrack TLEs). The periodic OOP updates are executed at 17:00 UTC and marked as black dotted vertical lines. The error in position is dominated by its tangential component, the error in velocity by its radial component.

The maximum error of the propagated with respect to the true position as well as the maximum position step occurring at execution of the OOP update are shown in Table 4 as a function of the chosen interval of OOP updates. An OOP update frequency of twice a day corresponds to the frequency of uplink possibilities during routine phase. This leads to a maximum position error of approximately 7 km in tangential direction. If the update frequency is reduced to only once per day or even every two days, due for example to ground station related problems, the maximum error increases to approximately 11 km and 21 km, respectively.

The maximum position jump occurs when the ground update of the OOP is executed and it results in a jump of the reference attitude computed on-board which must be compensated by the AOCS.

Table 4. Position Error in RTN-Frame depending on the OOP update frequency over a period of three days.

	OOP Update Frequency	R [km]	T [km]	N [km]
Maximum Error	Every two days	0.5	21.0	-0.1
	Once per day	0.5	11.4	0.9
	Twice per day	-0.4	7.0	-0.6
Maximum Jump during Update	Every two days	< 0.1	18.7	< 0.1
	Once per day	0.2	12.1	0.7
	Twice per day	0.2	8.1	0.3

The corresponding maximum error in velocity and the maximum jump during the update of a new OOP is shown in Table 5. An OOP update frequency of twice a day leads to a maximum velocity error of approximately 23 m/s in radial direction. The maximum velocity error in both the tangential and normal directions is smaller than 1 m/s.

Table 5. Velocity Error in RTN-frame depending on OOP update frequency over a period of three days.

	OOP Update Frequency	R [m/s]	T [m/s]	N [m/s]
Maximum Error	Every two days	23	1	2
	Once per day	13	1	1
	Twice per day	8	1	< 1
Maximum Jump during Update	Every two days	21	< 1	1
	Once per day	14	< 1	< 1
	Twice per day	9	< 1	< 1

4.3. Analysis of AOCS guidance angles based on OOP and TLEs updates

As described in section 2.1.2, in nominal science mode the satellites use the relative frame of reference for pointing their front-ends at each other. This is only possible when each satellite knows its own position, as described in the previous section, as well as the position of the partner satellite. The latter is calculated on board by propagating with a SGP4 algorithm the Two-Line-Elements uplinked every day.

Depending on the quality of the TLEs and the upload frequency, the pointing accuracy of both satellites varies in time. In this analysis, the acceptable angular error limits are determined by the ability of the Laser Ranging Interferometer to establish a link between both S/C. During a first signal acquisition, the LRI requires a pointing accuracy of approximately 300 µrad. Once the link has been established, in-orbit experience shows a tolerance of the LRI to deviations up to approximately 5 mrad, after which the lock status is lost.

The guidance angles (defined as the angles between the Relative Pointing Frame and Nadir Pointing Frame) and the pointing errors have been estimated over a time period of 5 days, for the case of a GPS outage (see Fig. 8). When daily OOP and TLEs updates are executed, the pointing errors remain within the 5 mrad tracking limit and mostly within the 300 µrad limit. After one day with no updates, the error in pitch direction exceeds the first acquisition limit. After three days without updates, the error in pitch exceeds the tracking limit. The error in yaw direction is significantly smaller than the one in pitch direction, the latter being caused by the high error in tangential direction described in the previous section.

The observed angle deviations are mainly due to the simplified gravitational model of the on-board propagator, together with the fact that the effect of the aerodynamic drag is not included. An overview of the maximum error, as well as the maximum jump, in pitch and yaw during the upload of OOP and TLE data is shown in Table 6.

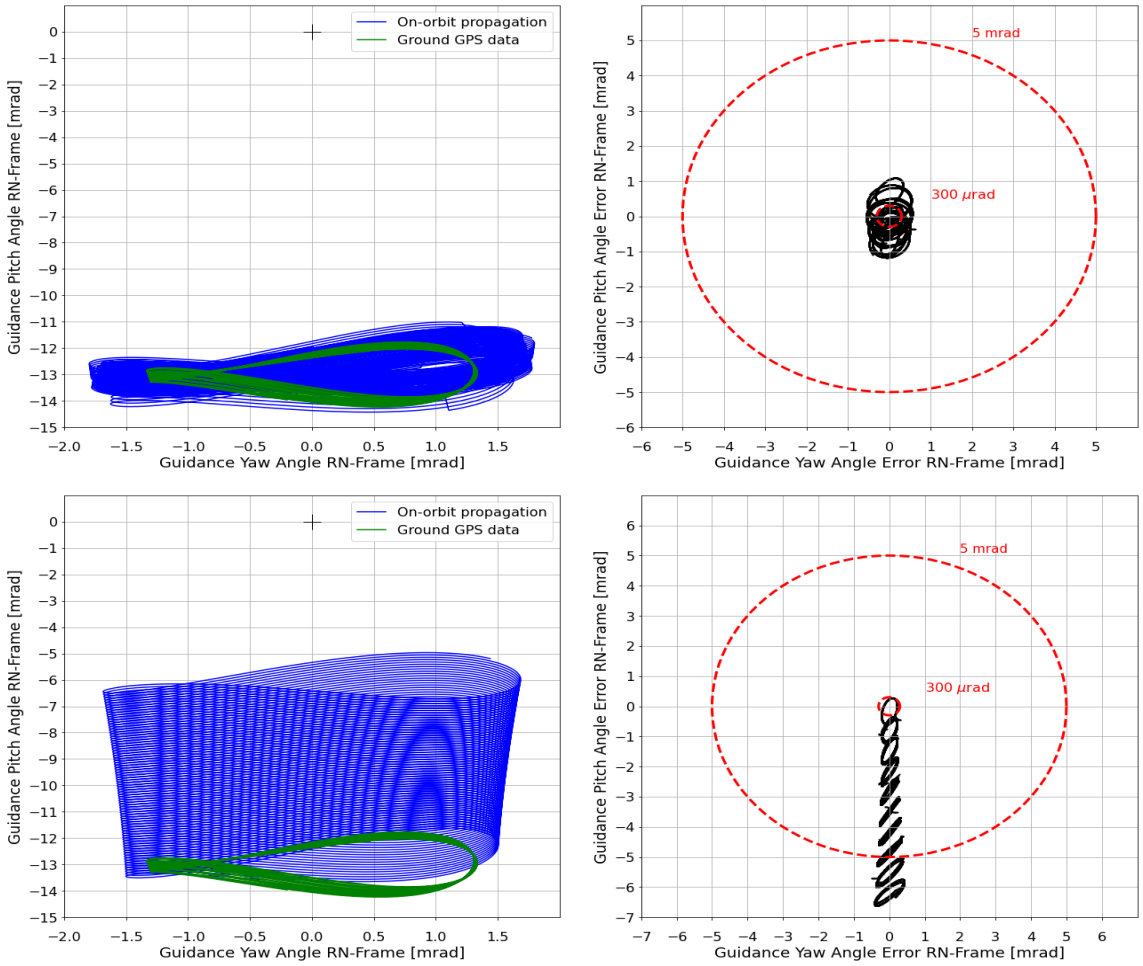

Fig. 8. On-board calculated guidance angles and pointing error relative to the other S/C over a time period of 5 days. The used RN frame describes the attitude difference between the relative frame and the nadir frame. The angles calculated from the on-board propagated data in case of a GPS outage are compared to those calculated from the nominal GPS measurement processing. The upper graphs are generated by applying ground updates twice a day. The lower graphs are generated assuming no update. Only few orbits are shown to improve clarity of the graphs.

Table 6 Maximum error and attitude jump in pitch and yaw depending on OOP and TLE update frequency, assuming the relative point frame of reference is active.

	OOP/TLE Update Frequency	Pitch [mrad]	Yaw [mrad]
Maximum Error	Every two days	3.2	0.5
	Once per day	2.0	0.6
	Twice per day	1.2	0.6
Maximum Jump during Update	Every two days	2.7	0.2
	Once per day	1.8	0.1
	Twice per day	1.2	0.1

This preliminary analysis indicates the possibility of performing AOCS and instrument operations in relative pointing even with no functional GPS receiver on one of the satellites. In a next step, the impact of different aerodynamic drag conditions as well as the long-term simulations including the variation of the β´ angle have to be analysed, to demonstrate the feasibility of this operational approach. The ability of the instruments to fulfil their performance requirements under these conditions must also be assessed.

5. Conclusions

The performance of the AOCS of the GRACE Follow-on satellites was stable over their first years in orbit, benefiting also from the lessons learned from the GRACE mission. With a remarkably low fuel consumption, the life expectancy based solely on the expenditure of this resource is a factor of ten higher than the initially planned mission duration of five years. A minor difference between the two tanks of the cold gas system has been observed on both satellites, but the uncertainties associated with the methods to estimate the remaining cold gas mass still have to be fully investigated.

The settings of the normal mode attitude controller were varied and several thruster tests carried out to help the science team calibrate the measurements of the accelerometer.

A method to bridge long phases without a functional GPS receiver has been developed and was used on one of the satellites for the several months in which the switch to the redundant instrument chain was prepared. During this time, however, the science data acquisition was interrupted. A preliminary analysis showed that the attitude pointing accuracy will be sufficient to support instrument operations in the worst-case scenario of the loss of the redundant chain. Further tests to improve on the performance will be needed in that case.

Acknowledgements

The Gravity Recovery and Climate Experiment Follow-on (GRACE-FO) mission is a partnership between NASA and the German Research Centre for Geosciences (GFZ). Mission Operations for the first 5 years are funded by GFZ and sub-contracted to DLR's German Space Operation Center (GSOC) in Oberpfaffenhofen.

The authors would like to thank the Science Data System teams at JPL and CSR for their help and fruitful discussions during the first years of life of the GRACE Follow-on satellites.

References

[1] B.D. Tapley, S. Bettadpur, M. Watkins, and C. Reigber, The Gravity Recovery and Climate Experiment: Mission Overview and Early Results, Geophysical Research Letters 31 (2004), Paper L09607.

[2] R.P. Kornfeld, B.W. Arnold, M.A. Gross, N.T. Dahya, W.M. Klipstein, P.F. Gath, and S. Bettadpur, GRACE-FO: The Gravity Recovery and Climate Experiment Follow-On Mission, Journal of Spacecraft and Rockets 56 (2019), 931-951.

[3] F.W. Landerer, F.M. Flechtner, H. Save, F.H. Webb, T. Bandikova, W.I. Bertiger et al., Extending the global mass change data record: GRACE Follow-On instrument and science data performance, Geophysical Research Letters 47 (2020), e2020GL088306.

[4] K. Abich, A. Abramovici, B. Amparan, A. Baatzsch, B. Bachman Okihiro, D. C. Barr et al., In-Orbit Performance of the GRACE Follow-on Laser Ranging Interferometer, Phys. Rev. Lett. 123 (2019), 031101.

[5] M. M. Witkowski, R. Gaston, M. Shirbacheh, GRACE Follow-On Early In-flight Challenges, in 16th International Conference on Space Operations, Cape Town, South Africa, 2021, 3 - 5 May.

[6] S. Löw, F. Cossavella, J. Herman, K. Müller, E. Davis, H. Save, Attitude and Orbit Control of the Grace Satellites at extremely low power, IAC-19-B.6.3.2, 70th International Astronautical Congress (IAC), Washington D.C., United States, 2019, 21 - 25 October.

[7] J. Herman , D. Presti, A. Codazzi and C. Belle, Attitude Control for GRACE, in ESA SP-548: 18th International Symposium on Space Flight Dynamics, Munich, Germany, 2004.

[8] Dr. K. Wirth, S. Löw, K. Müller, Dr. K. Snopek, R. Gaston, The challenge and consequences on mission operations after inverting a complex failure management concept in-orbit, SpaceOps-2021,3,x1438, 16th International Conference on Space Operations, Cape Town, South Africa, 2021, 3-5 May.

[9] F. Wang, S. Bettadpur, H. Save and G. Kruizinga, Determination of Center-of-Mass of Gravity Recovery and Climate Experiment Satellites, Journal of Spacecraft and Rockets 47 (2010), 371-379.

[10] F. Lex, Analyse von Anomalien innerhalb des Kaltgas-Systems der Low-Earth-Orbit Satellitenmission GRACE, Diploma Thesis, Hochschule München, 2015.

[11] C.M. McCullough, N. Harvey, H. Save, F.W. Landerer, F. Webb, Accelerometer Modeling and Calibrations for GRACE-FO, in AGU Fall Meeting Abstracts, 2019, G51B0590M.

[12] C. McCullough, N. Harvey, H. Save, T. Bandikova, Description of Calibrated GRACE-FO Accelerometer Data Products (ACT), 2019, JPL D-103863, NASA Jet Propulsion Laboratory, California Institute of Technology.

[13] Hoots Felix R., Roehrich Ronald L., Models for Propagation of NORAD Element Sets - Spacetrack rept. no. 3, Aerospace Defense Command - United States Air Force, 1980.

[14] S. Aida, M. Kirschner, M. Wermuth, R. Kiehling, Collision Avoidance Operations for LEO Satellites Controlled by GSOC, SpaceOps 2010, Huntsville, Alabama, 2010, 25.-29. April.